

## Competitive adsorption of Cd(II) and Pb(II) in aqueous solution onto humic acid derived from sewage sludge

Liang Dai<sup>a,\*</sup>, Weifan Zhao<sup>a</sup>, Gang Wang<sup>a</sup>, Bigui Wei<sup>a</sup>, Kang Zhang<sup>b</sup>, Tao Han<sup>a</sup>, Gui Ma<sup>c</sup>

<sup>a</sup>School of Environmental and Municipal Engineering, Lanzhou Jiaotong University, Lanzhou, China, Tel. +8613919353690, email: dailiang818@126.com (L. Dai), Tel. +8619893172530; email: 1448134537@qq.com (W. Zhao), Tel. +8618919181885; email: 11103615@qq.com (G. Wang), Tel. +8613919184748; email: 36935112@qq.com (B. Wei), Tel. +8618392658365; email: 1071437533@qq.com (T. Han)

<sup>b</sup>Jiangsu CRRC Environment Co., Ltd., Changshu, China, Tel. +8615095436119; email: 1060678975@qq.com

<sup>c</sup>Ningxia Normal University, Guyuan, China, Tel. +8613649536669; email: 403068067@qq.com

Received 15 February 2021; Accepted 27 July 2021

### ABSTRACT

Kinds of heavy metals often coexist in the actual contaminated wastewater, their competitive adsorption behavior could affect the adsorption capacity of adsorbents. In this paper, the sewage sludge-based humic acid (S-HA) was extracted from the excess sludge of a sewage treatment plant, the mutual effects and inner mechanisms of Cd(II) and Pb(II) adsorption in aqueous solution on S-HA were studied by single-metal and binary-metals systems. The results showed that the adsorption process for S-HA of Cd(II) and Pb(II) were fitted well by Langmuir and Freundlich adsorption models, the pseudo-second-order kinetic model can well fit the adsorption process of Cd(II) and Pb(II) by S-HA. In binary-metals system, Cd(II) and Pb(II) had competitive adsorption and the competitive ability of Pb(II) was stronger than Cd(II), which determined mainly by the electronegativity, hydrated ionic radius and charge to radius ratio. In binary-metals system, the Cd(II) adsorption on S-HA was inhibited, while the uptake of Pb(II) was not affected significantly. The adsorption capacities of Cd(II) and Pb(II) on S-HA increased with the increasing pH in binary-metal systems. When Cd(II) and Pb(II) coexisted, the adsorption capacities of two heavy metal ions were decreased compared with the single-metal adsorption system.

*Keywords:* Sludge; Humic acid; Cd(II); Pb(II); Competitive adsorption

### 1. Introduction

In recent years, with the rapid development of industrialization in China, a large number of pollutants such as wastewater and waste gas containing heavy metals have been discharged into the environment, causing serious environmental pollution. Heavy metals refer to metals with a relative density greater than or equal to 5.0 g/cm<sup>3</sup>. The common heavy metals are cadmium, chromium, mercury, silver, copper, lead and so on [1]. Heavy metal pollution refers to environmental pollution caused by toxic heavy

metals, mainly due to excessive heavy metals caused by industrial development, sewage irrigation and other processes. Heavy metals cannot be biodegraded and can enter the body of animals, plants and humans directly or indirectly through the food chain. After a long period of accumulation, they will seriously harm health [2,3]. Pan et al. [4] determined the contents of eight heavy metals in the soil of 32 cities in China and evaluated their effects on human health. The results showed that the average concentrations of these eight heavy metals were much higher than the background values of heavy metals in most cities, and the

\* Corresponding author.

ground accumulation index and enrichment factors showed moderate pollution level. It was suggested that lead, cadmium and hydrargyrum should be the priority heavy metal pollutants to be controlled. Lead is a poison of the central nervous system. When lead and its compounds enter the human body, it will cause damage to the body's immune system, hematopoiesis, nerves and other systems and tissue organ; cadmium (Cd) is a harmful element to the human body. When Cd enters the human body, it can form cadmium metallothionein in the body, reach the whole body through the blood, and selectively accumulate in the kidney and liver, which can cause harmful effects on the kidney and liver of the human body [5]. In recent years, a lot of heavy metal water pollution incidents have occurred in China, the heavy metal pollution incidents are often difficult to stop, which have caused serious harm to society. How to carry out pollution prevention and control of heavy metals is a search hotspot in many fields, such as environmental materials, ecological restoration, water treatment and so on. It is urgent to control heavy metal pollution.

At present, chemical precipitation and ion exchange resin method are the main methods for heavy metal wastewater treatment, but these two methods are complicated in management, high in processing cost [6]. The adsorption method has been used for removing heavy metals from aqueous solution by adsorption, chelation or ion coordination, which offers advantages such as wide source of adsorbents, high efficiency of heavy metals removal and ease of operation [7]. Many researches on the adsorption-desorption of heavy metals have been studied by scholars at home and abroad, but most of the research objects are biased towards a single heavy metal. The actual water environment is a mixed system of multiple heavy metal ions, with synergistic or antagonistic effects among various ions, which adsorption process is far more complicated than that of single heavy metal adsorption [8]. Less such researches on coexistence of competitive adsorption of multiple heavy metals have been studied currently, which seriously hinders the engineering adsorption treatment of actual heavy metal wastewater, so it is urgent to carry out targeted researches on competitive adsorption of various heavy metal ions.

Sludge is an inevitable by-product during wastewater treatment [9]. It is estimated that the annual sewage sludge production in China will reach 60 million tons by 2020 (moisture content 80%) [10]. Sludge contains toxic and harmful pollutants, which will harm the environment seriously if discharged without proper treatment. The treatment and disposal of sludge have become a serious environmental problem [11,12]. Sludge has a high content of organic substances (30%–70%). Traditional sludge disposal methods, such as sanitary landfill and incineration, will pose serious waste of organic resources in the sludge [13,14]. How to recycle sludge and dispose it harmlessly have become the hot topic of researches at present.

Humic acid (HA) is a main component of the organic matter in sludge. HA contains abundant active functional groups, such as phenolic hydroxyl groups, ketone groups, carboxyl groups, methoxy groups, etc which enable it to interact with heavy metal ions through mechanisms such as van der Waals forces, surface adsorption, complexation and so on [9]. HA was found to be a promising

environmental functional material for adsorbing heavy metal ions and has a strong binding ability to heavy metal ions [15]. At present, scholars at home and abroad have studied the HA more derived from minerals (such as lignite and weathered coal), soil and sediments as adsorption materials. However, the research on sludge-based humic acid (S-HA) has been rarely reported, mainly concentrated on the changes of humic acid composition and structure during sludge composting [16,17].

In this study, HA extracted from excess sludge of a sewage treatment plant was purified by alkali-extraction and acid-isolation method and characterized. Using S-HA as an adsorbent, the adsorption effect of Pb, Cd compound heavy metal pollutants from aqueous solution was studied by static adsorption experiments. The adsorption characteristics of Pb, Cd compound pollutants on S-HA were compared. The competitive adsorption law of Pb and Cd under coexisting conditions was explored, to evaluate the adsorption behavior of multiple heavy metals on the coexistence by S-HA, to provide theoretical basis and technical support for the application of S-HA in the removal of heavy metals, and also to provide a new approach of sludge resources for the utilization.

## 2. Materials and methods

### 2.1. Extraction and purification of S-HA

Experimental sludge was obtained from the concentration tank of the Anning Qilihe Sewage Treatment Plant in Lanzhou, China, which mainly receives urban domestic sewage. The sludge was placed in a cool and ventilated place to air-dry, then the dried sludge was ground and passed through a 100-mesh sieve. The extraction of S-HA was referred to the method recommended by the International Humic Substances Society (IHSS) [18].

### 2.2. Characterization of S-HA

The element composition of S-HA was measured by an elemental analyzer (Vario EL, Elementar, Germany); the surface functional groups were analyzed dosing an infrared-Raman spectrometer (VERTEX 70, Bruker, Germany); the surface morphology and microstructure of S-HA were investigated by cold field emission scanning electron microscope (JSM-6701F, JEOL, Japan); The specific surface area was measured from nitrogen adsorption data obtained from gas sorption analyzer (ASAP 2020, Micromeritics, U.S.). X-ray energy-dispersive spectroscopy (X-Max Extreme, Oxford, UK) and Field emission transmission electron microscope (TECNAIG2, FEI, USA), respectively.

### 2.3. Effect of pH on adsorption of Cd and Pb on S-HA

0.1 g S-HA was added into conical flasks with stoppers, and the mixed solution of Cd-Pb with a 20 mL concentration of 100 mg/L was prepared in each flask. The pH of mixed solution were adjusted to 2.0, 2.5, 3.0, 3.5, 4.0, 4.5, 5.0 and 5.5 using 0.1 mol/L HNO<sub>3</sub> or 0.1 mol/L NaOH solutions, respectively. Then the adsorption experiment was performed in an oscillating shaker operated at 180 rpm

and 25°C for 24 h. After shaking, the solution was filtered through a 0.45 µm membrane. The residual concentration of Cd(II) and Pb(II) in the filtrate was measured by atomic adsorption spectrophotometry (220FS, Varian, USA).

#### 2.4. Adsorption kinetics experiments

0.1 g S-HA was placed in a series of conical flasks with stoppers, 20 mL of heavy metal (single- or binary-) solution with a concentration of 100 mg/L was added to each flask, respectively. The concentrations of Cd(II) and Pb(II) in single-metal (Cd,Pb) and binary-metals systems (Cd-Pb) were both set as 100 mg/L, and the initial pH of the solution was adjusted to 5.0 by adding 0.1 mol/L HNO<sub>3</sub> or 0.1 mol/L NaOH solutions. The solution was shaken in an oscillating shaker at 180 rpm and 25°C for a period of time (0.3–24 h) and then analyzed the metal concentration.

The removal percentage and adsorption capacity of Cd(II) and Pb(II) were calculated by using Eqs. (1) and (2):

$$R(\%) = \frac{C_0 - C_e}{C_0} \quad (1)$$

$$q_e = \frac{(C_0 - C_e)V}{m} \quad (2)$$

where  $R$  represents the percentage of removal (%),  $C_0$  represents initial solution concentration of Cd(II) and Pb(II) (mg/L),  $C_e$  is the equilibrium concentration of Cd(II) and Pb(II) (mg/L),  $V$  is the volume of solution (L),  $q_e$  is the adsorption capacities of Cd(II) and Pb(II) at equilibrium (mg/g), and  $m$  is the weight of S-HA (g).

The pseudo-first-order kinetic equation, pseudo-second-order kinetic equation and intraparticle diffusion equation were respectively shown in Eqs. (3)–(5) as follows:

$$\frac{dq_t}{dt} = k_1(q_e - q_t) \quad (3)$$

$$\frac{dq_t}{dt} = k_2(q_e - q_t)^2 \quad (4)$$

$$q_t = k_d t^{1/2} + C_i \quad (5)$$

where  $q_e$  and  $q_t$  are the adsorption capacity of S-HA at adsorption equilibrium and at any time  $t$  (mg/L).  $k_1$  is the pseudo-first-order kinetic constant.  $k_2$  is the pseudo-second-order kinetic constant.  $k_d$  is the intra-particle diffusion rate constant. Intercept  $C_i$  is related to the thickness of the boundary layer. If  $C_i$  is not equal to zero, diffusion at the boundary layer towards the particle surfaces cannot be ignored. Additionally, the larger  $C_i$  is, the greater the influence of the boundary layer on adsorption.

#### 2.4. Isothermal adsorption experiments

The concentrations of Cd(II) and Pb(II) in single-metal(Cd,Pb) and binary-metals systems(Cd-Pb) were both set as

the same. Accurately weighed 0.1 g S-HA into 50 mL conical flasks with stoppers, and 20 mL mixed heavy metal solution with different concentration (10–200 mg/L) was added to each flask, respectively. The solution was shaken in an oscillating shaker at 180 rpm and 25°C for 24 h and then analyzed for metal concentrations. The removal percentage and adsorption capacities of Cd(II) and Pb(II) were calculated by using Eqs. (1) and (2).

The Langmuir equation, Freundlich equation, Temkin equation were respectively shown in Eqs. (6) and (7) as follows:

$$q_e = \frac{q_m K_L C_e}{1 + K_L C_e} \quad (6)$$

$$q_e = K_F C_e^{1/n} \quad (7)$$

where  $C_e$  represents the equilibrium solution concentration of metal (mg/L);  $q_e$  is the adsorption capacity of metal at equilibrium, (mg/g);  $K_L$  is the Langmuir adsorption constant, L/mg;  $q_m$  is the theoretical maximum adsorption capacity (mg/g);  $K_F$  is the Freundlich adsorption capacity parameter (L/mg);  $1/n$  is the Freundlich index, which reflects the ease of adsorption. When  $0.1 < 1/n < 1$ , the adsorption reaction was easy to proceed; when  $1/n > 2$ , adsorption was difficult to proceed.

Origin 8.1 software was used to process, fit and plot the experimental data. All of the experiments were performed in triplicate, the results took the average value.

### 3. Results and discussion

#### 3.1. Characterization of S-HA

##### 3.1.1. Elemental analysis

The chemical structure and functional group information of HA can be obtained by elemental composition analysis. The difference of structure and properties of HA could be obtained by calculating the atomic ratios of H/C, O/C and N/C [19,20]. The element composition of HA is listed in Table 1. The O/C atomic ratio of HA is usually used to indicate the content of oxygen-containing functional groups in HA. The O/C atomic ratio of S-HA extracted in this experiment was slightly higher than that of HA extracted from the compost of organic waste in urban greening by Zhang [21]. The H/C atomic ratio can be used to determine the aromaticity content of HA. The H/C atomic ratio in prepared S-HA was 1.79, indicating that S-HA had high aromaticity [22,23]. The C/N ratio of S-HA is related to its degree of humification [24]. The higher C/N ratio of S-HA, the lower the degree of humification. The C/N ratio in prepared S-HA

Table 1  
Elemental composition of S-HA

Elemental composition				Atomic ratio		
C/%	H/%	N/%	O/%	H/C	C/N	O/C
54.61	8.16	6.70	27.09	1.79	9.50	0.37

was 9.5, which was lower than that of HA produced during the composting process of Guo [25]. The HA extracted from this experiment had high degree of oxidation, aromaticity compared with HA extracted from different sources by other scholars.

### 3.1.2. Characteristics analysis of Fourier-transform infrared spectroscopy

The type and structure of the S-HA surface functional groups were identified using Fourier-transform infrared spectroscopy (FTIR) [26]. The FTIR spectra of S-HA are presented in Fig. 1. The peak appearing at the wavenumber of  $3,290\text{ cm}^{-1}$  is attributed to  $-\text{OH}$  stretching vibration of carboxyl groups and phenolic hydroxyl groups; the peak at  $2,924\text{ cm}^{-1}$  is assigned to the asymmetrical stretching vibration absorption peak of  $-\text{CH}_2$  in the aliphatic compounds,  $2,850\text{ cm}^{-1}$  corresponds to symmetrical stretching vibration peak of the  $-\text{CH}_2$  in the aliphatic compounds. These two strong absorption peaks indicated that high aliphatic carbon chain structures existed in HA. The strong absorption peaks at  $1,650$  and  $1,537\text{ cm}^{-1}$  are the stretching vibration peaks of the aromatic skeleton  $\text{C}=\text{C}$ , which indicate a high content of aromatic unsaturated substances existing in S-HA. The dense absorption peaks between  $1,540$  and  $1,510\text{ cm}^{-1}$  correspond to  $\text{N}-\text{H}$  deformation,  $\text{C}-\text{N}$  stretching and aromatic  $\text{C}=\text{C}$  stretching. The peak at  $1,236\text{ cm}^{-1}$  was the absorption peak of  $\text{C}-\text{O}$  connected to the ester and phenolic hydroxyl. The vibration peak at  $1,038\text{ cm}^{-1}$  is  $\text{C}-\text{O}-\text{C}$ . It can be inferred from the FTIR analysis that the surface of S-HA contained a large number of oxygen-containing functional groups, such as carboxy, alcohol hydroxyl and phenolic hydroxyl groups, and also had aromatic and aliphatic compounds. Furthermore, S-HA had a high content of aromatic structure. The existence of these surface functional groups provided a basis for the adsorption of  $\text{Cd}(\text{II})$  and  $\text{Pb}(\text{II})$  by S-HA.

After  $\text{Cd}^{2+}$  adsorption, the peak of  $-\text{OH}$  in S-HA at  $3,290\text{ cm}^{-1}$  moved to  $3,296\text{ cm}^{-1}$ , and the peak intensity decreased obviously, which indicated that  $-\text{OH}$  in S-HA

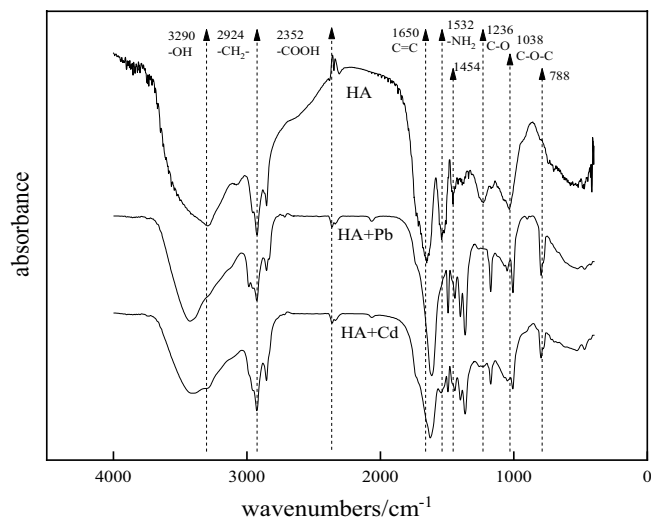


Fig. 1. FTIR spectra of S-HA before and after adsorption of  $\text{Cd}^{2+}$  and  $\text{Pb}^{2+}$ .

complexed with  $\text{Cd}^{2+}$ . After adsorption, the stretching vibration peak of aromatic ring skeleton  $\text{C}=\text{C}$  at  $1,650\text{ cm}^{-1}$  moved to  $1,622\text{ cm}^{-1}$ , and the absorption peak near  $1,236\text{ cm}^{-1}$  weakened obviously, indicating that the aromatic ring and phenolic hydroxyl groups in S-HA participated in the adsorption reaction. The change of dense absorption peaks was the most obvious between  $1,532$  and  $1,329\text{ cm}^{-1}$ , which indicated that alcohol, carboxylic acid and phenolic functional groups participated in the adsorption reaction.

Before and after  $\text{Pb}^{2+}$  adsorption, the intensity and shape of several absorption peaks in infrared spectrum changed greatly. The absorption peak in the range of  $1,650$ – $1,236\text{ cm}^{-1}$  showed that aromatic ring, carboxyl and hydroxyl on the surface of S-HA were involved in the adsorption of  $\text{Pb}^{2+}$ . The absorption peak of  $-\text{COOH}$  at  $2,352\text{ cm}^{-1}$  also changed greatly, which indicated that carboxylic acid functional groups participated in the adsorption reaction. After adsorption, the migration degree and peak intensity of  $-\text{OH}$  peak at  $3,290\text{ cm}^{-1}$  changed greatly, which indicated that  $\text{Pb}^{2+}$  and  $-\text{OH}$  had complexation.

### 3.1.3. Surface characterizations and micromorphology

The scanning electron microscopy-energy-dispersive X-ray spectroscopy (SEM-EDS) and transmission electron microscopy (TEM) spectrogram of S-HA are shown in Fig. 2. The surface of S-HA is loosely clustered with an underdeveloped pore structure. The elemental composition of the S-HA surface was analyzed by EDS, and S-HA was mainly composed of C, N, O, S and P. Cd and Pb elements of S-HA were not identified by EDS analysis before adsorption. As can be seen from TEM spectra, S-HA has a flaky structure with a clearly defined texture.

The surface area, pore volume and pore size were determined by the  $\text{N}_2$  adsorption–desorption isotherm at  $77\text{ K}$ . Prior to measurement, the samples were outgassed at  $40^\circ\text{C}$  for 2 h. The specific surface area of S-HA was calculated by Brunauer–Emmett–Teller (BET) method, and the pore size distribution was calculated by Barrett–Joyner–Halenda (BJH) method. The specific surface area, total pore volume and average pore size of S-HA were  $0.9782\text{ m}^2/\text{g}$ ,  $0.002763\text{ cm}^3/\text{g}$  and  $32.32\text{ nm}$ , respectively. According to IUPAC classification [27], the  $\text{N}_2$  adsorption–desorption isotherms of S-HA correspond to a similar Type II isotherm (Fig. 3), which indicated that S-HA is a typical physical adsorption process on nonporous or macroporous adsorbents. S-HA had a small specific surface area, undeveloped pore structure, and the pore size distribution is mainly macropore.

### 3.2. Effect of pH on adsorption of $\text{Cd}(\text{II})$ and $\text{Pb}(\text{II})$ by S-HA

The effect of solution pH on the adsorption of  $\text{Cd}(\text{II})$  and  $\text{Pb}(\text{II})$  by S-HA under competitive adsorption system is shown in Fig. 4. It can be seen that solution pH has a great influence on adsorption. With the increase of pH value, the equilibrium adsorption capacity ( $q_e$ ) of S-HA for the two metals increased continuously and reached the maximum value when pH value was 5.0. The adsorption capacity of S-HA on Pb was much higher than that on Cd. The adsorption capacity of S-HA for  $\text{Cd}(\text{II})$  and  $\text{Pb}(\text{II})$  was higher under the high solution pH, which was due to the

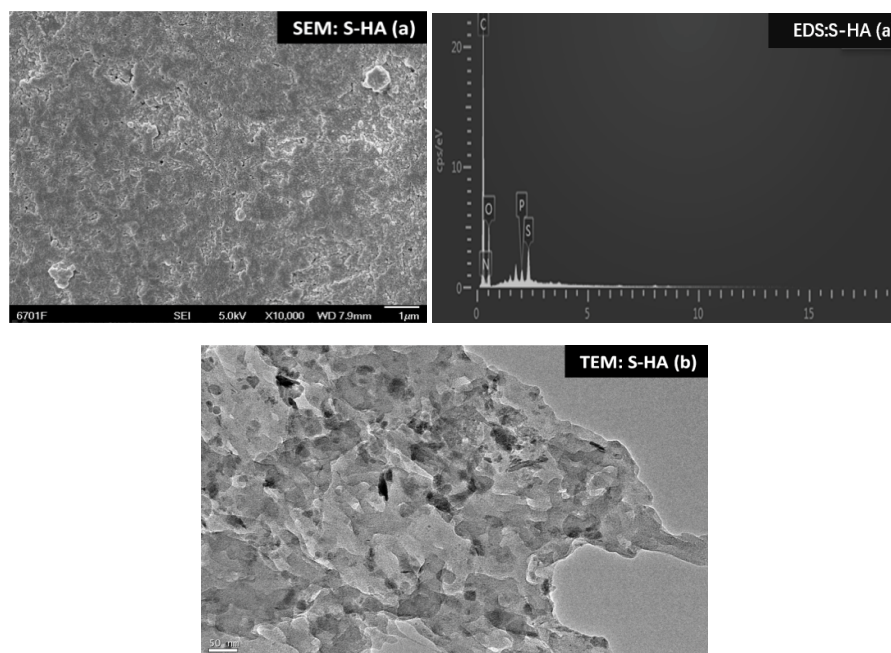


Fig. 2. SEM image and EDS spectra (a) and TEM spectra (b) of S-HA.

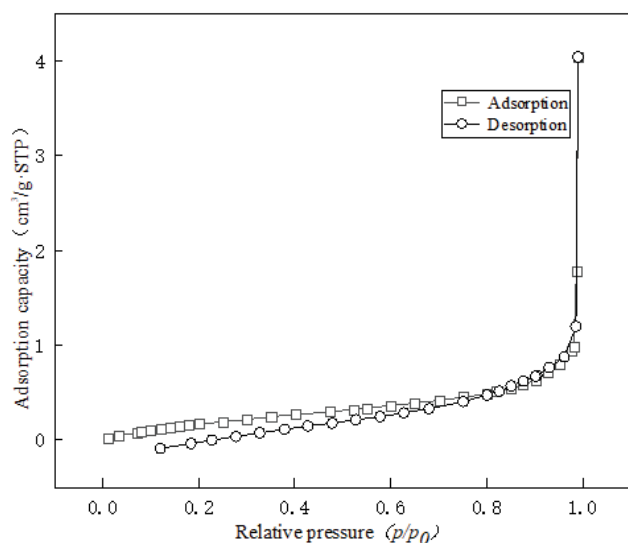


Fig. 3.  $N_2$  adsorption–desorption isotherm of purified S-HA.

high  $H^+$  concentration in the solution occupying part of the adsorption sites on S-HA when the pH value was low, thus generating competitive adsorption with Cd(II) and Pb(II), restraining the adsorption of S-HA for Cd(II) and Pb(II). When the solution pH increased, the  $H^+$  concentration and the surface negative charge of S-HA increased, the electrostatic attraction of Cd(II), Pb(II) and S-HA increased, as well as the adsorption capacities of S-HA for Cd(II) and Pb(II).

### 3.3. Kinetics study of Cd(II) and Pb(II) adsorption on S-HA in the single-metal and binary-metals systems

It can be observed from Fig. 5 that the adsorption capacities of Cd(II) and Pb(II) increased rapidly in the initial

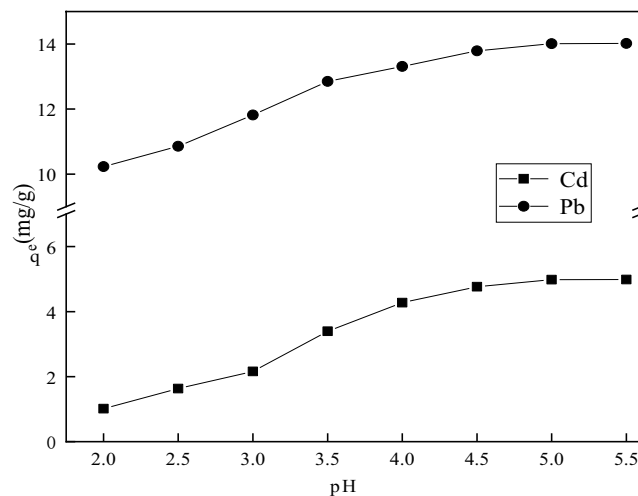


Fig. 4. Effect of solution pH on adsorption of Cd(II) and Pb(II) by S-HA.

adsorption stage of single-metal and binary-metals systems, this stage was mainly surface adsorption; the heavy metal ions diffused into the interior of S-HA after 2 h with the adsorption capacity increased slowly, eventually reached the adsorption equilibrium. In the initial stage of adsorption, many adsorption sites were in the system and the concentration of heavy metal ions in the solution was high, as well as the mass transfer driving force, so the adsorption rate was faster. As the adsorption proceeded, the concentration of ions in the solution and the mass transfer driving force decreased, as well as the adsorption rate. The adsorption equilibrium time of Pb(II) was approximately the same in single and binary adsorption systems. The adsorption equilibrium time of Cd(II) in binary system was shorter than

that in single system, indicating that the presence of Pb(II) made the reaction time between S-HA and Cd(II) shorter, and sped up the time for Cd(II) to reach the adsorption equilibrium. The S-HA exhibited higher adsorption capacity for Pb(II) compared to that for Cd(II) in single and binary adsorption systems.

The pseudo-first-order model and the pseudo-second-order model were applied to fit the experimental data to study the rate reached the adsorption equilibrium state of Cd(II) and Pb(II) adsorption on S-HA. In addition, the

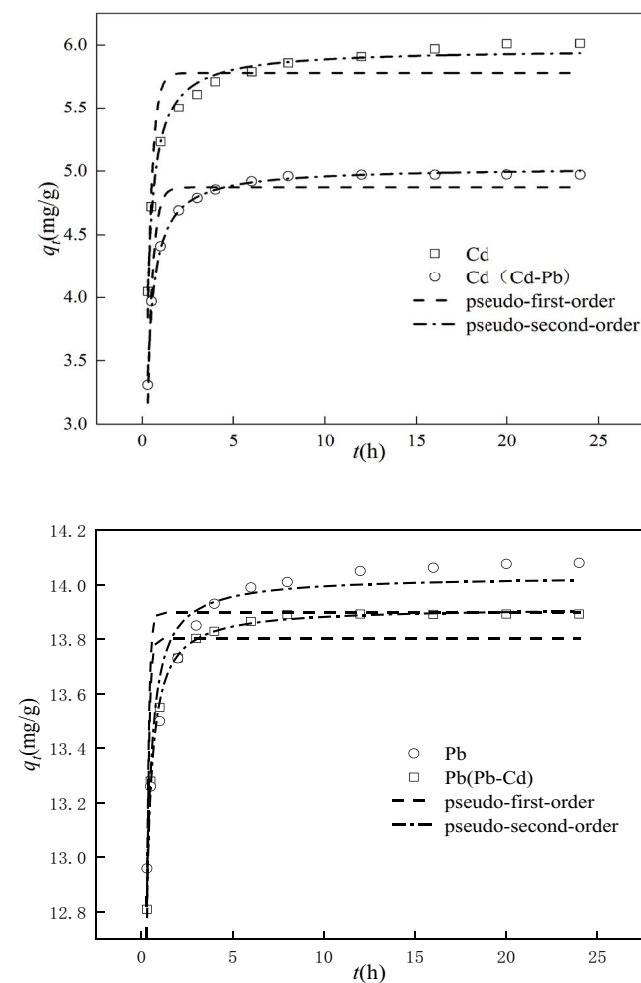


Fig. 5. Kinetic data and fitting curves of Cd(II) and Pb(II) adsorbed on S-HA in the single- and binary-metals systems.

Table 2

Kinetic fitting parameters of Cd(II) and Pb(II) adsorbed on S-HA in the single- and binary-metal systems

Adsorption system	Pseudo-first-order model			Pseudo-second-order model		
	$q_e$	$k_1$	$R^2$	$q_e$	$k_2$	$R^2$
Cd	5.78	3.64	0.88	5.97	1.18	0.99
Cd(Cd-Pb)	4.87	3.50	0.93	5.03	1.36	0.99
Pb	13.90	8.54	0.64	14.03	2.60	0.95
Pb(Pb-Cd)	13.80	8.46	0.82	13.92	2.82	0.99

competitive mechanism of Pb(II) and Cd(II) on S-HA was explored. As seen in Table 2, the pseudo-second-order model is more accurate to describe the adsorption process in either single-metal system or binary-metals systems, the theoretical adsorption capacity  $q_e$  obtained by fitting in the pseudo-second-order model was basically consistent with the experimental data, the adsorption mechanism was mainly attributed to the chemical adsorption, with the complexation reaction of oxygen-containing functional groups in S-HA with heavy metal ions. Physical adsorption did not play a leading role in the adsorption process because of the small specific surface area and less pore structure of S-HA. The  $q_e$  of Pb(II) were both larger in the binary-metals and single-metal adsorption systems. The  $q_e$  of Cd(II) and Pb(II) were both lower in the binary-metals systems than in the single-metal system, suggesting that the competitive adsorption effect was obvious. The  $k_2$  value for Pb(II) were larger than that for Cd(II) in the binary-metals system, implying that the adsorption rate of Pb(II) was faster than that of Cd(II). The  $k_2$  values were larger in the binary-metals system than in the single-metal system, which indicated that the presence of the coexisting heavy metal ions could produce different degree effects on the adsorption rate of the Cd(II) and Pb(II) by S-HA. That was due to the competition effect between Cd(II) and Pb(II) changed the adsorption rate of the two heavy metal ions.

According to the fitting curves of the intra-particle diffusion equation (Fig. 6) and the fitting data table (Table 3), the adsorption process of Cd(II) and Pb(II) on S-HA in the binary-metals and single-metal adsorption systems could be divided into two stages. The first stage was the diffusion of Cd(II) and Pb(II) in solution was transferred to the S-HA surface (liquid membrane diffusion phase); The second stage was that the diffusion of Cd(II) and Pb(II) was transferred to S-HA internal pores (intra-particle diffusion stage). The diffusion rate constant relationship was  $k_{d1} > k_{d2}$  ( $k_{d1}$  is the rate constant of intra-particle diffusion in the first stage,  $k_{d2}$  is the rate constant of intra-particle diffusion in the second stage), which indicated that the diffusion process of liquid membrane was very fast. Linear fitting extension lines shown in Fig. 6 did not pass through the origin, indicating that intra-particle diffusion was not the only rate-limiting step in the adsorption process.

#### 3.4. Thermodynamic study of Cd(II) and Pb(II) adsorbed on S-HA in the single- and binary-metals systems

The adsorption isotherms of Cd(II) and Pb(II) adsorbed on S-HA are shown in Fig. 7. The adsorption data were fitted

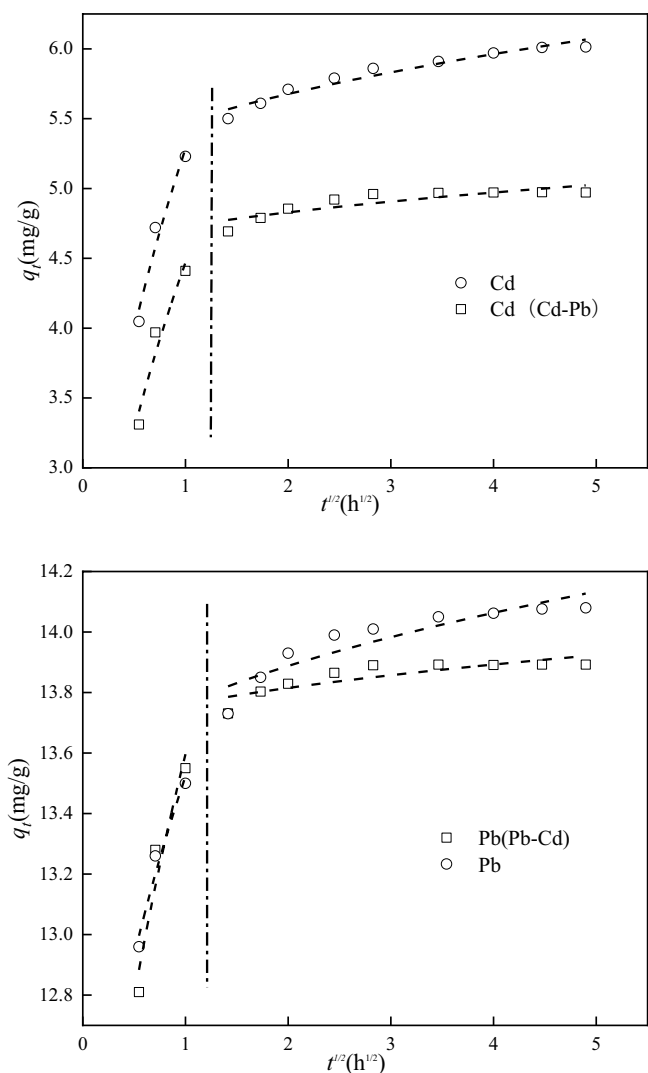


Fig. 6. Intraparticle diffusion fitting of Cd(II) and Pb(II) adsorbed on S-HA in the single- and binary-metals systems (a) Stage 1 and (b) Stage 2.

Table 3  
Fitting parameters of intra-particle diffusion kinetic of Cd(II) and Pb(II) adsorbed on S-HA in the single- and binary-metal systems

Adsorption system	$k_{d1}$	$C_1$	$R^2$	$k_{d2}$	$C_2$	$R^2$
Cd(Cd-Pb)	4.10	0.37	0.94	0.24	4.49	0.76
Pb	2.03	11.50	0.96	0.30	13.47	0.84
Pb(Pb-Cd)	2.74	10.85	0.92	0.13	13.63	0.73

by Freundlich, Langmuir and Temkin isothermic adsorption models, respectively. When Cd(II) and Pb(II) coexisted, the adsorption capacities of two heavy metal ions decreased relative to the single adsorption system. The theoretical maximum adsorption capacities of S-HA for Cd(II) and Pb(II) were 14.89 and 26.60 mg/g, respectively (Table 4). These were

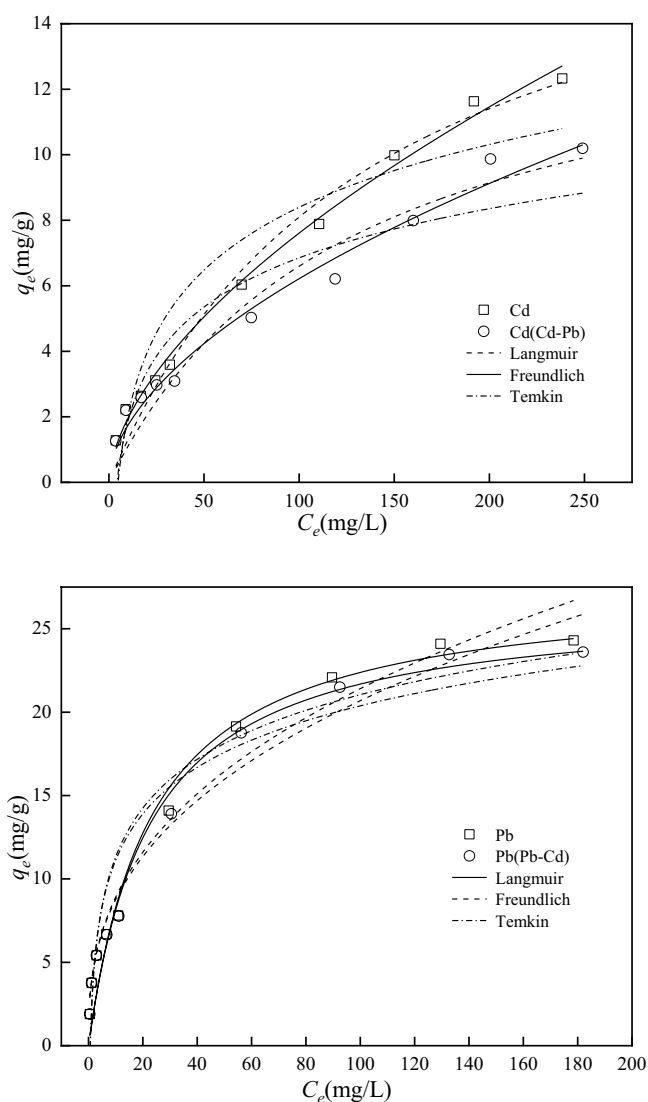


Fig. 7. Isotherms and fitting curves of Cd(II) and Pb(II) adsorbed on S-HA in single- and binary-metals systems.

Table 4  
Isothermal adsorption fitting parameters of Cd(II) and Pb(II) adsorbed on S-HA in single- and binary-metal systems

Adsorption system	Langmuir model			Freundlich model		
	$q_m$	$K_L$	$R^2$	$K_F$	$1/n$	$R^2$
Cd	19.29	0.007	0.98	0.500	0.59	0.99
Pb	27.59	0.043	0.98	3.712	0.38	0.98
Cd(Cd-Pb)	14.89	0.008	0.95	0.486	0.55	0.98
Pb(Cd-Pb)	26.59	0.044	0.97	3.705	0.37	0.98

due to the certain number of adsorption sites for S-HA, and the competition between two heavy metal ions for a limited adsorption sites made the adsorption capacity decreased. When the equilibrium concentration of heavy metal ions was low in the binary-metals systems, the competitive adsorption was not obvious, because the adsorption sites in the

Table 5

Comparison of the maximum monolayer adsorption capacity of various adsorbents were tabulated

No.	Heavy metal	Adsorbents	$q_m$ (mg/g)	References
1	Pb <sup>2+</sup>	<i>Lemna gibba</i>	4.22	[27]
2	Pb <sup>2+</sup>	Zeolite	14.2	[28]
3	Pb <sup>2+</sup>	Pod husk	4.83	[29]
4	Pb <sup>2+</sup>	Lipopeptides modified Na-montmorillonite	20.3	[30]
5	Cd <sup>2+</sup>	Lipopeptides modified Na-montmorillonite	19.5	[30]
6	Pb <sup>2+</sup>	Mercaptoethanol-modified silica	10.42	[31]
7	Cd <sup>2+</sup>	Mercaptoethanol-modified silica	4.75	[31]
8	Cd <sup>2+</sup>	SH-SiO <sub>2</sub>	13.87	[32]
9	Pb <sup>2+</sup>	SH-SiO <sub>2</sub>	18.48	[32]

Table 6

Physical and chemical parameters of heavy metal ions

Heavy metal	Ion radius (Å)	Electronegativity	Hydration energy (kJ/mol)	Hydrolysis constant pK <sub>1</sub>	Effective ionic radius (nm)	Hydrated ion radius (nm)
Cd	0.97	1.69	1,806	7.78	0.097	0.426
Pb	1.19	2.33	1,500	11.70	0.266	0.401

adsorption system were sufficient at the low equilibrium concentration, and the competition between two ions on the adsorption sites was not intense. A large number of heavy metal ions competed for limited adsorption sites, and the competition of Cd(II) and Pb(II) increased with the increasing equilibrium concentration. A comparison of the maximum monolayer adsorption capacity of various adsorbents are tabulated in Table 5 [28–33].

The competitive adsorption process could be well fitted by both Langmuir and Freundlich models, indicating that the competitive adsorption process existed in both chemical and physical adsorption. At the same time, it also showed that under the competitive condition, the adsorption of the two ions on the monolayer chemisorption also had the presence of multiple molecular layers of physico-chemical adsorption. According to the Langmuir model, the theoretical maximum adsorption capacities of S-HA for Cd(II) and Pb(II) in single adsorption system was 19.29 and 27.59 mg/g, respectively;  $K_f$  can be used to evaluate the adsorption capacity, the Freundlich model fitting parameters  $K_f$  were 0.50 L/mg and 3.71 L/mg, respectively, suggesting that the adsorption capacities of S-HA on the two heavy metal ions were Pb(II) > Cd(II), which were consistent with the results of adsorption kinetics analysis. The adsorption capacities of two ions in the single system were both larger than that of the competitive adsorption system, the S-HA presented higher adsorption capacity for Pb(II) compared to that for Cd(II) in the competitive adsorption system by comparing the results in the single and competitive adsorption experiments. The adsorption process was  $0.1 < 1/n < 1$ , which showed that S-HA had good adsorption effect on two heavy metal ions in the single system and competitive adsorption system.

### 3.5. Selectivity of Cd(II) and Pb(II) in competitive adsorption

Although both Cd(II) and Pb(II) are divalent metal ions, the adsorption properties of S-HA for the two ions were significantly different. This was due to the difference in the characteristics of two metals and the affinity of adsorption sites were different, and the physical and chemical properties of the two ions are shown in Table 6. Both ion radius and ion charge had effects on the adsorption process, and the adsorption performance of heavy metal ions increased with the increasing ion radius [34]. The ionic charges of Cd(II) and Pb(II) are the same, but the effective ionic radius of Pb(II) was larger than Cd(II), and Pb(II) had higher electronegativity than Cd(II), which made Pb(II) easier to form stable complexes with unshared pair electrons in O atom on S-HA [35]. Therefore, the adsorption amount of Pb(II) by S-HA was higher than that of Cd(II). The affinity of heavy metal ions to the adsorbent was also related to the hydration energy of the heavy metal ions and the radius of the hydration ions. The lower the hydration energy, the easier it be to remove the surface hydration water and hydrolyze into free ions in the adsorption process [36]. The hydration ion radius and hydration energy of Pb(II) were lower than those of Cd(II), and the hydroxyl compound formed after hydrolysis of Pb(II) had higher adsorption affinity with S-HA, so Pb with lower hydration energy was easy to dehydrate and coordinate into Pb(II) ions to adsorbed on the surface of S-HA.

## 4. Conclusion

The results of characterization showed that S-HA was mainly composed of C, H, O and N, the surface has loose clusters, under developed pore structure, small specific

surface area. It contained a large number of oxygen-containing functional groups, such as carboxyl groups, phenolic hydroxyl groups, with high aromaticity and more fat chain structure.

In the competitive adsorption system, the solution pH had a great influence on the adsorption. Freundlich and Langmuir models can provide the better fit for the adsorption process. The theoretical maximum adsorption capacity of S-HA for Cd(II) and Pb(II) in single adsorption system was 19.29 and 27.59 mg/g, respectively. The adsorption of two kinds of ions in single and competitive adsorption systems were mainly attributed to the chemical adsorption, physical adsorption also took effect. Intra-particle diffusion was not the only speed control step in the adsorption process, and the adsorption amount of Pb(II) was greater than Cd(II) whether in single-metal or binary-metals systems.

The analysis results of metal characteristics showed that the selective adsorption coefficient of Pb(II) in the competitive adsorption system was larger than that of Cd(II), Pb(II) could be favorably adsorbed with stronger competitive adsorption capacity, which determined mainly by the electro negativity, hydrated ionic radius and charge to radius ratio. When Cd(II) and Pb(II) coexisted, the adsorption capacity of S-HA to two heavy metal ions decreased compared with the single adsorption system.

#### Acknowledgements

The authors acknowledge the financial support of the Natural Science Foundation of Gansu province (20JR10RA236), Ningxia Autonomous Region Higher School Scientific Research Program (NGY2018-117) and the University's Innovation Ability Improvement Project of Gansu Provincial office of Education (2019B-051).

#### References

- [1] Y.-Y. Wang, Y.-X. Liu, H.-H. Lu, R.-Q. Yang, S.-M. Yang, Competitive adsorption of Pb(II), Cu(II), and Zn(II) ions onto hydroxyapatite-biochar nanocomposite in aqueous solutions, *J. Solid State Chem.*, 261 (2018) 53–61.
- [2] F.J. Cao, C. Lian, J.G. Yu, H.J. Yang, S. Lin, Study on the adsorption performance and competitive mechanism for heavy metal contaminants removal using novel multi-pore activated carbons derived from recyclable long-root *Eichhornia crassipes*, *Bioresour. Technol.*, 276 (2019) 211–218.
- [3] G. Wu, H.B. Kang, X.Y. Zhang, H.B. Shao, L.Y. Chu, C.J. Ruan, A critical review on the bio-removal of hazardous heavy metals from contaminated soils: Issues, progress, eco-environmental concerns and opportunities, *J. Hazard. Mater.*, 174 (2010) 1–8.
- [4] L. Pan, Y. Wang, J. Ma, Y. Hu, B. Su, G. Fang, L. Wang, B. Xiang, A review of heavy metal pollution levels and health risk assessment of urban soils in Chinese cities, *Environ. Sci. Pollut. Res.*, 25 (2017) 1055–1069.
- [5] H. Wang, X.Z. Yuan, Y. Wu, H.J. Huang, G.M. Zeng, Y. Liu, X.L. Wang, N.B. Lin, Y. Qi, Adsorption characteristics and behaviors of graphene oxide for Zn(II) removal from aqueous solution, *Appl. Surf. Sci.*, 279 (2013) 432–440.
- [6] X.M. Gao, Y. Zhang, Y. Dai, F. Fu, High-performance magnetic carbon materials in dye removal from aqueous solutions, *J. Solid State Chem.*, 239 (2016) 265–273.
- [7] H. Xu, H.F. Yuan, J.G. Yu, S. Lin, Study on the competitive adsorption and correlational mechanism for heavy metal ions using the carboxylated magnetic iron oxide nanoparticles (MNP-COOH) as efficient adsorbents, *Appl. Surf. Sci.*, 473 (2019) 960–966.
- [8] X.C. Chen, G.C. Chen, L.G. Chen, Y.X. Chen, J. Lehmann, M.B. McBride, A.G. Hay, Adsorption of copper and zinc by biochars produced from pyrolysis of hardwood and corn straw in aqueous solution, *Bioresour. Technol.*, 102 (2011) 8877–8884.
- [9] Z.M. Gusiati, D. Kulikowska, B. Klik, Suitability of humic substances recovered from sewage sludge to remedy soils from a former as mining area – a novel approach, *J. Hazard. Mater.*, 338 (2017) 160–166.
- [10] B. Dong, X.G. Liu, L.L. Dai, X.H. Dai, Changes of heavy metal speciation during high-solid anaerobic digestion of sewage sludge, *Bioresour. Technol.*, 131 (2013) 152–158.
- [11] L.L. Wei, K.N. Qin, Q.L. Zhao, K. Wang, F.T. Kabutay, F.Y. Cui, Utilization of artificial recharged effluent for irrigation: pollutants removal and risk assessment, *J. Water Reuse Desal.*, 7 (2017) 77–87.
- [12] D. Xue, X.D. Huang, The impact of sewage sludge compost on tree peony growth and soil microbiological, and biochemical properties, *Chemosphere*, 93 (2013) 583–589.
- [13] G. Yang, G.M. Zhang, H.C. Wang, Current state of sludge production, management, treatment and disposal in China, *J. Water Res.*, 78 (2015) 60–73.
- [14] P. Manara, A. Zabaniotou, Towards sewage sludge based biofuels via thermochemical conversion – a review, *Renewable Sustainable Energy Rev.*, 16 (2012) 2566–2582.
- [15] B.A.G. Melo, F.L. Motta, M.H.A. Santana, Humic acids: structural properties and multiple functionalities for novel technological developments, *Mater. Sci. Eng., C*, 62 (2016) 967–974.
- [16] S.Y. Li, D.Y. Li, J.J. Li, G.X. Li, B.X. Zhang, Evaluation of humic substances during co-composting of sewage sludge and corn stalk under different aeration rates, *Bioresour. Technol.*, 245 (2017) 1299–1302.
- [17] C.S. Zhang, Y. Xu, M.H. Zhao, H.W. Rong, K.F. Zhang, Influence of inoculating white-rot fungi on organic matter transformations and mobility of heavy metals in sewage sludge based composting, *J. Hazard. Mater.*, 344 (2018) 163–168.
- [18] R.S. Swift, Chapter 35 – Organic Matter Characterization, D.L. Sparks, A.L. Page, P.A. Helmke, R.H. Loeppert, P.N. Soltanpour, M.A. Tabatabai, C.T. Johnston, M.E. Sumner, Eds., *Methods of Soil Analysis: Part 3 Chemical Methods*, 5.3, 1996.
- [19] Z. Yang, M.C. Du, J. Jiang, Reducing capacities and redox potentials of humic substances extracted from sewage sludge, *Chemosphere*, 144 (2016) 902–908.
- [20] G. Yamin, M. Borisover, E. Cohen, J.V. Rijn, Accumulation of humic-like and proteinaceous dissolved organic matter in zero-discharge aquaculture systems as revealed by fluorescence EEM spectroscopy, *Water Res.*, 108 (2016) 412–421.
- [21] L. Zhang, X.Y. Sun, Addition of seaweed and bentonite accelerates the two-stage composting of green waste, *Bioresour. Technol.*, 243 (2017) 154–162.
- [22] C. Plaza, N. Senesi, G. Brunetti, D. Mondelli, Evolution of the fulvic acid fractions during co-composting of olive oil mill wastewater sludge and tree cuttings, *Bioresour. Technol.*, 98 (2007) 1964–1971.
- [23] F. Barje, L. El Fels, H. El Hajjoui, S. Amir, P. Winterton, M. Hafidi, Molecular behaviour of humic acid-like substances during co-composting of olive mill waste and the organic part of municipal solid waste, *Int. Biodeterior. Biodegrad.*, 74 (2012) 17–23.
- [24] X.Q. Wang, H.Y. Cui, J.H. Shi, Y. Zhao, Z.M. Wei, Relationship between bacterial diversity and environmental parameters during composting of different raw materials, *Bioresour. Technol.*, 198 (2015) 395–402.
- [25] X.X. Guo, H.T. Liu, Z.Z. Chang, X.P. Tao, H.M. Jin, H.M. Dong, Z.P. Zhu, Review of humic substances developed in organic waste aerobic composting and its agronomic effect, *J. Ecol. Rural Environ.*, 34 (2018) 489–498.
- [26] E. Smidt, K. Meissl, The applicability of Fourier-transform infrared (FTIR) spectroscopy in waste management, *Waste Manage.*, 27 (2007) 268–276.
- [27] K.S.W. Sing, D.H. Everett, R.A.W. Haul, L. Moscou, R.A. Pierotti, J. Rouquerol, T. Siemieniowska, Reporting physisorption data

- for gas solid systems with special reference to the determination of surface-area and porosity (recommendations 1984), *Pure Appl. Chem.*, 57 (1985) 603–619.
- [28] M.D.C. Carreno-De Leon, N. Flores-Alamo, M. Jose Solache-Rios, I. de la Rosa-Gomez, G. Diaz-Campos, Lead and copper adsorption behaviour by *Lemna gibba*: kinetic and equilibrium studies, *Clean – Soil Air Water*, 45 (2017) 1600357.1–1600357.12.
- [29] P.K. Pandey, S.K. Sharma, S.S. Sambhi, Removal of lead(II) from waste water on zeolite-NaX, *J. Environ. Chem. Eng.*, 3 (2015) 2604–2610.
- [30] A.I. Obike, J.C. Igwe, C.N. Emeruwa, K.J. Uwakwe, Equilibrium and kinetic studies of Cu(II), Cd(II), Pb(II) and Fe(II) adsorption from aqueous solution using cocoa (*Theobroma cacao*) pod husk, *J. Appl. Sci. Environ. Manage.*, 22 (2018) 182–190.
- [31] Z. Zhu, C. Gao, Y.L. Wu, L.F. Sun, X.L. Huang, W. Ran, Q.R. Shen, Removal of heavy metals from aqueous solution by lipopeptides and lipopeptides modified Na-montmorillonite, *Bioresour. Technol.*, 147 (2013) 378–386.
- [32] A. Kořak, A. Lobnik, M. Bauman, Adsorption of mercury(II), lead(II), cadmium(II) and zinc(II) from aqueous solutions using Mercapto-modified silica particles, *Int. J. Appl. Ceram. Technol.*, 12 (2015) 461–472.
- [33] R. Rostamian, M. Najafi, A.A. Rafati, Synthesis and characterization of thiol-functionalized silica nano hollow sphere as a novel adsorbent for removal of poisonous heavy metal ions from water: kinetics, isotherms and error analysis, *Biochem. Eng. J.*, 171 (2011) 1004–1011.
- [34] Z. Mahdi, Q.J. Yu, A.E. Hanandeh, Competitive adsorption of heavy metal ions (Pb(II), Cu(II), and Ni(II)) onto date seed biochar: batch and fixed bed experiments, *Sep. Sci. Technol.*, 54 (2019) 888–901.
- [35] C.C. Ding, W.C. Cheng, X.X. Wang, Z.Y. Wu, Y.B. Sun, C.L. Chen, X.K. Wang, S.H. Yu, Competitive sorption of Pb(II), Cu(II) and Ni(II) on carbonaceous nanofibers: a spectroscopic and modeling approach, *J. Hazard. Mater.*, 313 (2016) 253–261.
- [36] M.S. Berber-Mendoza, J.I. Martínez-Costa, R. Leyva-Ramos, H.J.A. Garcia, N.A.M. Castillo, Competitive adsorption of heavy metals from aqueous solution onto oxidized activated carbon fiber, *Water Air Soil Pollut.*, 229 (2018) 1–15.